

## SCHEDULE RISK COUPLING ANALYSIS OF MEGAPROJECTS BASED ON N-K MODEL AND SYSTEM DYNAMICS

Zuosen ZhANG<sup>1</sup>, Jianwen HUANG<sup>2</sup>, Xingxia WANG<sup>3\*</sup>, Jianjun ZHANG<sup>4\*</sup>,  
Jianfu ZHOU<sup>5\*</sup>, Yufeng WANG<sup>6\*</sup>

*This study develops a model to analyze schedule risk coupling in diversion tunnels. Using the work breakdown structure (WBS)- risk breakdown structure (RBS) method, four primary risk categories- human, machine and materials, environment, and management- were identified. System dynamics (SD) and the N-K model, with parameters derived from Monte Carlo simulations, were then used to quantify coupling effects. A case study on a hydropower project confirms that coupling severity escalates with the number of interacting risks. Notably, the analysis reveals that couplings between subjective factors (human, management) and operational factors (machine and materials) are the most critical sources of delay. The proposed model offers a practical framework for managers to proactively identify and mitigate these high-risk combinations.*

**Keywords:** risk coupling, tunnel construction, schedule risk, N-K Model, megaprojects.

### 1. Introduction

Hydropower development serves as a strategic pillar for China's energy transition and carbon neutrality goals. Most hydropower megaprojects in China are situated in the Alpine Gorges region, face unique schedule risks from compressed timelines and geological complexity. Particularly in diversion tunnels, hydrological volatility and terrain constraints amplify flood risks during construction. Therefore,

---

<sup>1</sup> Hubei Key Laboratory of Construction and Management in Hydropower Engineering, China Three Gorges University, China, e-mail: nathan0219@qq.com

<sup>2</sup> PhD, Prof., Hubei Key Laboratory of Construction and Management in Hydropower Engineering, China Three Gorges University, China, e-mail: jwhuang@ctgu.edu.cn

<sup>3\*</sup> PhD, Associate Prof., Hubei Key Laboratory of Construction and Management in Hydropower Engineering, China Three Gorges University, China, e-mail: xxwang@ctgu.edu.cn, (corresponding author)

<sup>4</sup> \* Chief Economic Officer, China Gezhouba Group No.1 Engineering Co., Ltd., China, e-mail: 447689662@qq.com, (corresponding author)

<sup>5\*</sup> PhD, Lecturer, Hubei Key Laboratory of Construction and Management in Hydropower Engineering, China Three Gorges University, China, e-mail: zhoujianfu@ctgu.edu.cn, (corresponding author)

<sup>6\*</sup> PhD, Lecturer, Hubei Key Laboratory of Construction and Management in Hydropower Engineering, China Three Gorges University, China, e-mail: yfwang@ctgu.edu.cn, (corresponding author)

it is necessary to comprehensively analyze the schedule risk of the hydropower megaproject.

Schedule delays typically result from coupling interactions among four risk dimensions: Human ( $M_1$ ), Machine and Materials ( $M_2$ ), Environment (E), and Management ( $M_3$ ). The occurrence of schedule delays is often caused by the interaction and joint coupling of multiple risk factors. Therefore, analyzing schedule risks from a multi-factor coupling perspective is essential to uncover the mechanisms and effects of risk interactions and enhance schedule risk control. This study analyzes the construction and schedule risk characteristics of diversion tunnels, identifies the schedule risk factors by using the work breakdown structure (WBS)- risk breakdown structure (RBS) method, reveals the coupling relationships through system dynamics (SD) model, calculates the coupling effect with the N-K model, and simulates the schedule risk by using the Monte Carlo method.

Diversion tunnels, as deeply buried structures, face high risks due to challenging environments. Existing risk models address specific uncertainties: Afshar et al. [1] optimized dam flood costs under hydraulic uncertainty, while Sari et al. [2] quantified risks via time-series decomposition. Prior studies have developed diverse risk assessment approaches. Fouladgar et al. [3] pioneered fuzzy-technique for order of preference by similarity to ideal solution (TOPSIS) integration for tunnel collapse risk evaluation, while Monte Carlo simulations [4-6], fuzzy set [7-9], fault tree [10-12], and grey system [13] are also commonly used. Recent advances include Ji et al. [14]'s fuzzy analytic hierarchy process (FAHP)-based bridge risk analysis and Duressa et al. [15]'s hydraulic flood modeling.

Recent advancements in schedule risk management demonstrate methodological diversification. Xu et al. [16] pioneered a cost-schedule integration model for complex systems, employing system simulations for validation. Concurrently, Wu et al. [17] developed AI-driven real-time control systems for urban rail transit schedules, while C.Z. Li et al. [18] innovatively combined social network analysis with building information modeling (BIM) technology to map hypertext preprocessor network risks and optimize stakeholder communication under critical schedule constraints. Cross-disciplinary explorations of risk coupling mechanisms reveal three key trends: 1) Theoretical frameworks emphasizing supervision roles [19] and multi-model integration [20]; 2) Quantitative methodologies including class-attribute interaction theory [21] and terrain-specific risk indices [22]; 3) Predictive applications such as concrete cracking models under multi-factor coupling [23]. Current research predominantly focuses on safety risk quantification through variable interaction analysis [24, 25], yet critical gaps persist in hydropower megaprojects where interdependent risk factors systematically amplify delays. This limitation underscores the urgent need for dedicated investigation into schedule risk coupling mechanisms to enable proactive delay prevention.

Current risk coupling research spans disasters, safety, economics, environment, and weapon systems. For hydropower megaprojects, schedule risk coupling is nascent. However, interactions among risk factors may alter schedule outcomes. Therefore, studying schedule risk coupling is conducive to exploring the risk coupling mechanism and effect between risk factors, avoiding risk coupling events from the source, and thus reducing the risk of project delay.

The remainder of this paper is organized as follows. Section 2 details the research methodology, using the WBS-RBS method to identify risk factors and system dynamics to qualitatively analyze their coupling mechanisms. Section 3 establishes quantitative models: a physics-based model for homogeneous coupling and the N-K model for heterogeneous coupling, supported by Monte Carlo simulations. Section 4 presents a case study of a diversion tunnel, analyzing results for both coupling scenarios. Finally, Section 5 concludes the paper, summarizing the key findings and contributions.

## 2. Research methodology

### 2.1. Identification of schedule risk factors

As the basis for schedule risk coupling analysis, timely identification of diverse risk factors is essential for diversion tunnel construction—a complex system where progress risks correlate closely with environmental and operational conditions. While various identification methods exist, including checklists, Delphi, and fault tree analysis (FTA), this study adopts the WBS-RBS approach for its systematic nature (Fig. 1).

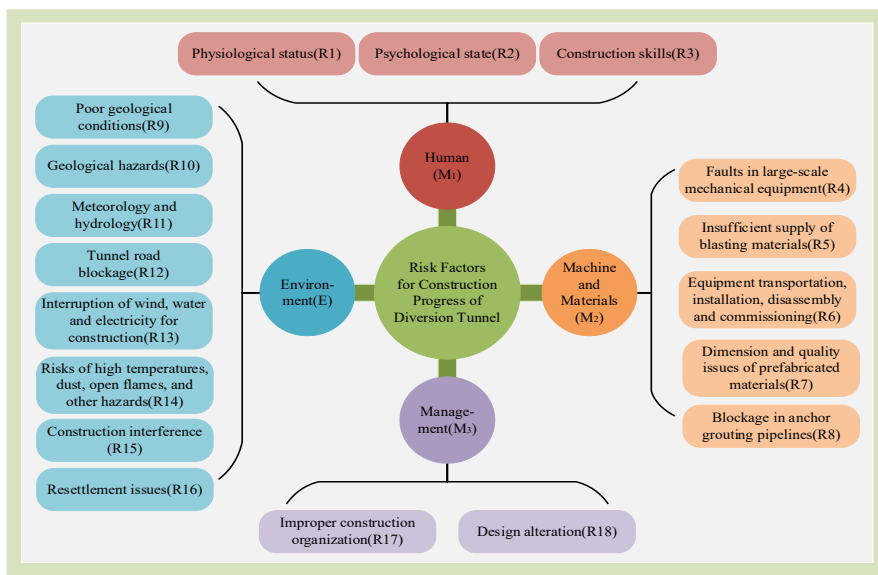


Fig. 1. RBS decomposition structure of construction schedule

Based on the characteristics of the diversion tunnel's workflow, the project is divided into relatively independent engineering units for schedule and risk analysis. Using WBS structure of the project, risk factors were systematically categorized to create RBS. The RBS framework comprehensively accounts for the impacts of Human ( $M_1$ ), Machine and Materials ( $M_2$ ), Environment (E), and Management ( $M_3$ ) on the schedule. Consequently, risk factors are classified into four categories based on their sources. The WBS decomposition layer serves as the row vector, while the RBS risk factor layer functions as the column vector. This approach helps analyzing the impact of risk factors and identifying progress risks.

## 2.2. Mechanism of schedule risk coupling

"Coupling" denotes interactions and mutual influences between systems, while "risk coupling" describes interactions among risk factors in complex activities that alter overall risk outcomes. Risk coupling manifests as three types: "negative/zero coupling" (reduced/unchanged risk, acceptable for control) when factors coordinate, and "positive coupling" (increased risk with severe consequences, unacceptable) when factors reinforce each other. In construction schedules, positive coupling of schedule risk factors inevitably exacerbates adverse impacts, necessitating clear understanding for effective control.

During the execution of the project, the construction system itself has certain defensive capabilities, that is, it will not have a vital impact on the construction period, and the construction managers will also actively prevent the occurrence of risks. However, the system's defenses capabilities have a threshold. If a single risk factor or combined coupling risks surpass it, the system will be adversely affected. Taking the construction progress of the diversion tunnel as an example, when the role of risk factors exceeds the threshold, the construction schedule will be delayed. Fig. 2 depicts the coupling mechanism for the diversion tunnel's construction schedule risk.

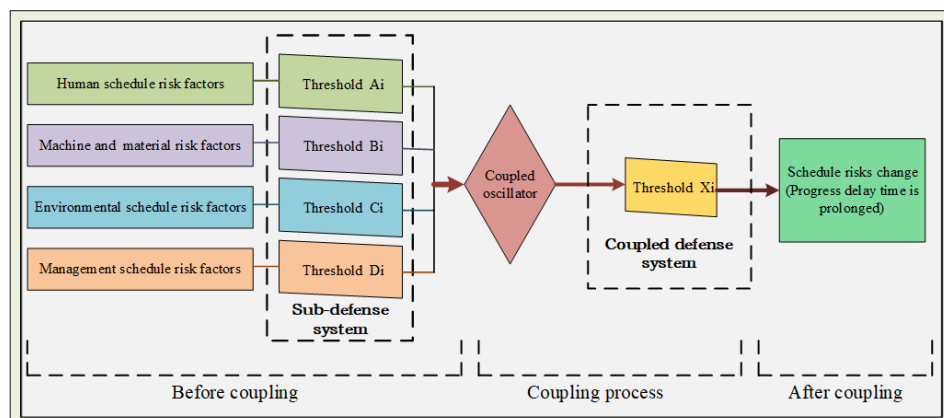


Fig. 2. Coupling mechanism of diversion tunnel schedule risk

### 2.3. Analysis of the coupling relationship of construction schedule risk based on system dynamics

The diversion tunnel construction schedule risk system is an open system with highly overlapping subsystems and multiple feedback complex relationships. Thus, a SD model is suitable for analyzing this system. First, the SD causality feedback diagram was constructed to qualitatively describe and analyze the nonlinear coupling relationships within the construction schedule risk system. Next, the WBS-RBS matrix was used to identify potential coupling among risk factors. Arrow lines in the system indicate coupling, with positive feedback representing the promotion, induction, or amplification of risk factors. This method provides a quantitative depiction of the relationships between subsystems in system. The feedback graph of the coupling relationship is shown in Fig. 3.

Risk coupling is categorized based on variable sources into homogeneous single-factor coupling and heterogeneous multi-factor coupling.

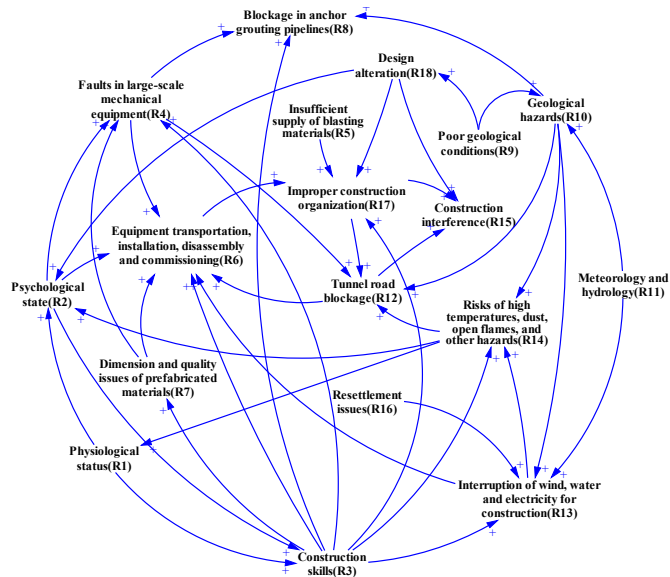


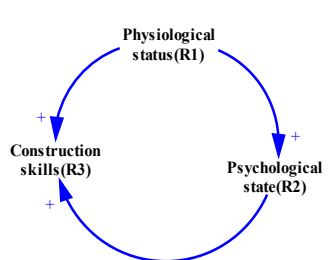
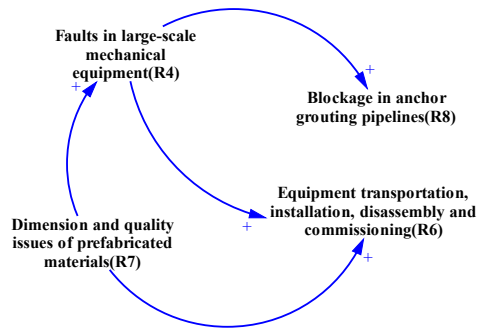
Fig. 3. Feedback graph of coupling relationships of construction schedule risk system

#### 2.3.1. Homogeneous single-factor coupling

Homogeneous single-factor coupling in diversion tunnel construction refers to interactions among risk elements within the same category (e.g., M<sub>1</sub>-M<sub>1</sub>, M<sub>2</sub>-M<sub>2</sub>, E-E, M<sub>3</sub>-M<sub>3</sub>).

(1) The internal coupling of Human (M<sub>1</sub>). Diversion tunnel construction involves personnel risks including illness, fatigue, safety awareness deficiencies, and insufficient experience. These are categorized as physiological status (R1),

psychological state (R2), and construction skills (R3). R1 directly affects R3 or indirectly influences R3 via R2 (Fig. 4).

Fig. 4. The coupling relationships of M<sub>1</sub>Fig. 5. The coupling relationships of M<sub>2</sub>

(2) The internal coupling of Machine and Materials (M<sub>2</sub>). Machine risks involve equipment risks include faults in large-scale mechanical equipment (R4), delays during equipment transportation, installation, disassembly, and commissioning (R6). Material risks include raw material shortages, the dimension and quality issues of prefabricated materials (R7), and the quality problem of finished products (e.g., blockage in anchor grouting pipeline R8). While most exhibit coupling relationships, blasting material shortages (R5) are primarily driven by external market factors with minimal internal coupling (Fig. 5).

(3) The internal coupling of Environment (E). The environmental risk factors of construction sites include natural, site operation and social context risk factors. Physical environment factors (e.g., R11), and social factors (e.g., R16) can be coupled with operational factors (e.g., R13), increasing safety hazards. In diversion tunnels, natural environmental risks exhibit higher frequency and severity than social risks (Fig. 6).

(4) The internal coupling of Management (M<sub>3</sub>). Management risks (e.g., improper construction organization R17, design alterations R18) directly or indirectly affect project progress. Design alterations (R18) critically influence construction organization, with coupling mechanisms shown in Fig. 7.

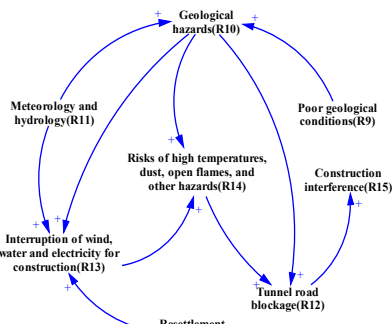


Fig. 6. The coupling relationships of E

Fig. 7. The coupling relationship of M<sub>3</sub>

### 2.3.2. Heterogeneous multi-factor coupling

Heterogeneous multi-factor coupling refers to interactions between risk elements across two or more categories, including 11 types: M<sub>1</sub>-M<sub>2</sub>, M<sub>1</sub>-E, M<sub>1</sub>-M<sub>3</sub>, M<sub>2</sub>-E, M<sub>2</sub>-M<sub>3</sub>, E-M<sub>3</sub>, M<sub>1</sub>-M<sub>2</sub>-E, M<sub>1</sub>-M<sub>2</sub>-M<sub>3</sub>, M<sub>1</sub>-E-M<sub>3</sub>, M<sub>2</sub>-E-M<sub>3</sub>, M<sub>1</sub>-M<sub>2</sub>-E-M<sub>3</sub>.

(1) M<sub>1</sub>-M<sub>2</sub> coupling: The M<sub>2</sub> in the construction period is entirely managed by M<sub>1</sub>, creating an inseparable bidirectional influence.

(2) M<sub>1</sub>-E coupling: M<sub>1</sub> are primarily influenced by on-site operational environments rather than natural/social factors. For instance, the on-site environment directly impacts R3, subsequently affecting R1 and R2.

(3) M<sub>1</sub>-M<sub>3</sub> coupling: Management risks (R17 and R18) are closely tied to M<sub>1</sub>. These factors trigger coupling effects by altering managerial decision-making and mindset.

(4) M<sub>2</sub>-E coupling: Natural environmental factors strongly influence M<sub>2</sub>, while M<sub>2</sub> interacts with on-site environmental risks. For example, R13 may exacerbate R6, causing schedule disruptions.

(5) M<sub>2</sub>-M<sub>3</sub> coupling: M<sub>2</sub> has an impact on M<sub>3</sub>, and R5 or equipment issues can disrupt construction organization and cause delays.

(6) E-M<sub>3</sub> coupling: E interact with M<sub>3</sub>. For instance, environmental hazards may require R18, whereas R17 exacerbates on-site risks (e.g., traffic congestion due to coordination failures).

Diversion tunnel schedules are susceptible to multi-factor chain reactions (e.g., M<sub>1</sub>-M<sub>2</sub>-E, M<sub>1</sub>-M<sub>2</sub>-M<sub>3</sub>, M<sub>1</sub>-E-M<sub>3</sub>, M<sub>2</sub>-E-M<sub>3</sub>). Full-scale coupling (M<sub>1</sub>-M<sub>2</sub>-E-M<sub>3</sub>), though rare, typically leads to severe accidents.

## 3. Model

### 3.1. Homogeneous single-factor coupling model

According to synergy theory, the coupling influence and coordination level determine the system's transition from disorder to order. A coupling model quantifies interactions between system elements, while the coupling degree reflects synergy levels. The synergy among ordered parameters drives the system's transition from disorder to order and governs its characteristics and evolution.

Construction schedules are influenced by multiple risk factors, whose interactions generate dynamic coupling effects. In physics, coupling strength ( $qd_{ij}$ ) measures interactions between risk factors. The coupling strength indicates the influence of schedule risk factor  $R_j$  on  $R_i$ . A higher  $qd_{ij}$  value denotes stronger influences. The efficiency coefficients  $u_j$  (for  $R_j$ ) and  $u_i$  (for  $R_i$ ) characterize risk factor interactions. The coupling strength is calculated as follow.

$$qd_{ij} = [(u_i \times u_j) / (u_i + u_j)^2]^{\frac{1}{2}} = \frac{\sqrt{u_i u_j}}{u_i + u_j} \quad (1)$$

The efficiency coefficient is determined based on the upper and lower limits of schedule risk levels:

$$u_i = \begin{cases} (e_i - \alpha_i) / (\beta_i - \alpha_i), & u_i \text{ is a positive efficacy} \\ (\beta_i - e_i) / (\beta_i - \alpha_i), & u_i \text{ is a negative efficacy} \end{cases} \quad (2)$$

where,  $e_i$  is the expected risk value of risk factor  $R_i$ ;  $\alpha_i$  and  $\beta_i$  are the lower and upper limits of the risk value for  $R_i$ , respectively.

### 3.2. Heterogeneous multi-factor coupled with N-K model

The N-K model originated from information theory to quantify information measurement and transmission, later evolving into a standard framework for analyzing complex dynamic systems. The model is defined by two central parameters: N, which represents the number of components in a system, and K, which denotes the degree of interconnectedness, meaning the number of other components that influence the fitness contribution of each component.

The diversion tunnel schedule risk coupling system is a large-scale complex system encompassing heterogeneous multi-risk coupling scenarios. Each risk category comprises multiple factors, generating diverse coupling scenarios via combinatorial interactions. The N-K model constructs the tunnel's risk coupling framework, where N denotes four subsystems: human ( $M_1$ ), machine and materials ( $M_2$ ), environment (E) and management ( $M_3$ ). K represents interaction quantities between subsystems within the underground powerhouse schedule risk system. Coupling is categorized as partial (2 to n-1 risk categories) or full (n categories), depending on whether subsystems exceed their risk containment thresholds. The N-K model quantifies subsystem interactions. A permutation's coupling value escalates with interaction intensity, reflecting elevated risk. The full coupling formula (all four risk types interacting) is:

$$T_4(M_1 \cdot M_2 \cdot E \cdot M_3) = \sum_{h=1}^H \sum_{i=1}^I \sum_{j=1}^J \sum_{k=1}^K P_{h,i,j,k} \log_2(P_{h,i,j,k} / (P_{h..} \cdot P_{i..} \cdot P_{..j} \cdot P_{...k})) \quad (3)$$

where  $h=1, \dots, H$ ;  $i=1, \dots, I$ ;  $j=1, \dots, J$ ;  $k=1, \dots, K$ ,  $P_{h,i,j,k}$  represents the probability of coupled risk occurrence when the four categories of risks- $M_1$ ,  $M_2$ , E, and  $M_3$ -are in state  $h$ ,  $i$ ,  $j$  and  $k$  respectively.

In most cases, coupling involves three (not all four) risk categories, termed local coupling with four types. Their risk calculation formulas are as follows.

$$T_{31}(M_1 \cdot M_2 \cdot E) = \sum_{h=1}^H \sum_{i=1}^I \sum_{j=1}^J P_{h,i,j} \log_2(P_{h,i,j} / (P_{h..} \cdot P_{i..} \cdot P_{..j})) \quad (4)$$

$$T_{32}(M_1 \cdot M_2 \cdot M_3) = \sum_{h=1}^H \sum_{i=1}^I \sum_{k=1}^K P_{h,i,k} \log_2(P_{h,i,k} / (P_{h..} \cdot P_{i..} \cdot P_{...k})) \quad (5)$$

$$T_{33}(M_1-E-M_3) = \sum_{h=1}^H \sum_{j=1}^J \sum_{k=1}^K P_{h,j,k} \log_2(P_{h,j,k} / (P_{h\dots} \cdot P_{\dots j} \cdot P_{\dots k})) \quad (6)$$

$$T_{34}(M_2-E-M_3) = \sum_{i=1}^I \sum_{j=1}^J \sum_{k=1}^K P_{i,j,k} \log_2(P_{i,j,k} / (P_{i\dots} \cdot P_{\dots j} \cdot P_{\dots k})) \quad (7)$$

Local coupling includes both dual-category (e.g., M<sub>2</sub>-E interactions causing delays) and three-category risk combinations, totaling six permutations with corresponding formulas.

$$T_{21}(M_1-M_2) = \sum_{h=1}^H \sum_{i=1}^I P_{h,i} \log_2(P_{h,i} / (P_{h\dots} \cdot P_{\dots i})) \quad (8)$$

$$T_{22}(M_1-E) = \sum_{h=1}^H \sum_{j=1}^J P_{h,j} \log_2(P_{h,j} / (P_{h\dots} \cdot P_{\dots j})) \quad (9)$$

$$T_{23}(M_1-M_3) = \sum_{h=1}^H \sum_{k=1}^K P_{h,k} \log_2(P_{h,k} / (P_{h\dots} \cdot P_{\dots k})) \quad (10)$$

$$T_{24}(M_2-E) = \sum_{i=1}^I \sum_{j=1}^J P_{i,j} \log_2(P_{i,j} / (P_{i\dots} \cdot P_{\dots j})) \quad (11)$$

$$T_{25}(M_2-M_3) = \sum_{i=1}^I \sum_{k=1}^K P_{i,k} \log_2(P_{i,k} / (P_{i\dots} \cdot P_{\dots k})) \quad (12)$$

$$T_{26}(E-M_3) = \sum_{j=1}^J \sum_{k=1}^K P_{j,k} \log_2(P_{j,k} / (P_{\dots j} \cdot P_{\dots k})) \quad (13)$$

After determining schedule risk impact distributions, Monte Carlo simulations model the total diversion tunnel duration probability distribution and completion likelihood under risk factors. For single risk factor  $R_n$ , the actual construction period  $T_n$  equals the planned period  $T_0$  plus the influence  $t(x_{mn})$  of on process.

$$T_n = T_0 + \sum_{m=1}^k t(x_{mn}) \quad (14)$$

where,  $n$  is the index for the specific risk factor  $R_n$ ;  $m$  is the index for a construction process; and  $t(x_{mn})$  represents the time delay on process  $m$  caused by the impact variable  $x_{mn}$  from risk factor  $R_n$ .

Schedule risk quantifies the probability of exceeding specified timelines, and it can be calculated as below:

$$R = 1 - P(T \leq T^*) \quad (15)$$

where  $R$  = schedule risk, and  $P(T \leq T^*)$  = probability of completion within the specified time  $T^*$ .

In the Monte Carlo simulations, planned durations of each diversion tunnel process are input. Delay probability distributions are assigned to risk-affected processes based on risk-construction process correlations. Through preset simulation iterations, total construction duration is calculated with critical path monitoring, thereby obtaining the required data: probability distribution, mean value, confidence interval, completion probability and progress indicators. In the flowchart,  $N$  represents the total number of preset simulation iterations, and  $n$  is the current iteration counter (Fig. 8).

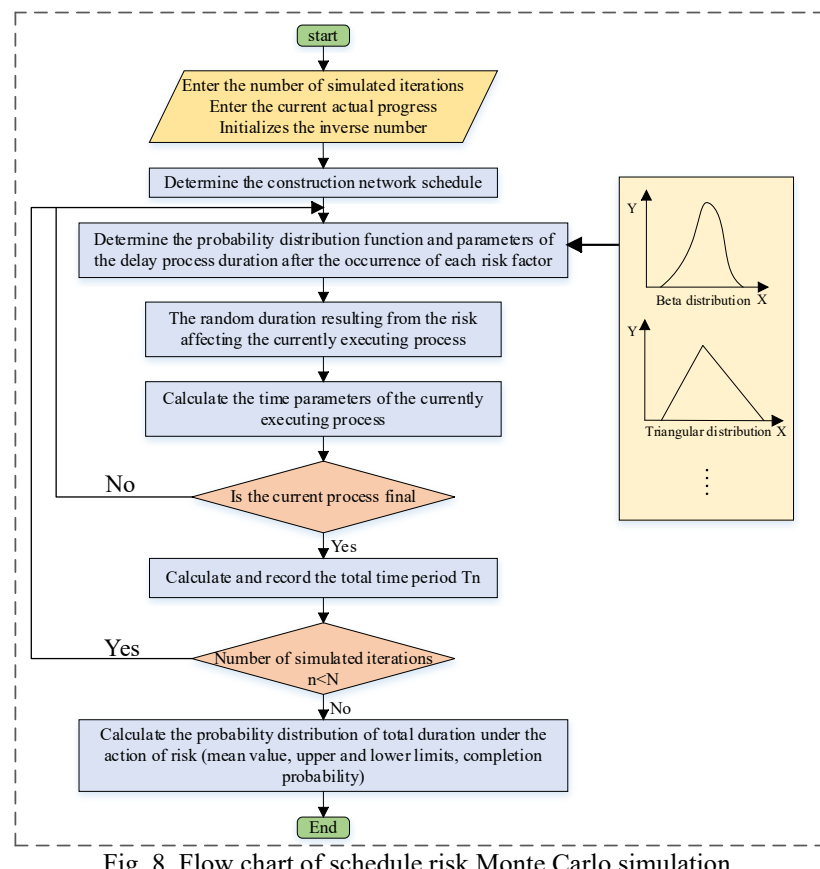


Fig. 8. Flow chart of schedule risk Monte Carlo simulation

#### 4. Results and discussion

The cascade hydropower project comprises a hyperbolic arch dam (crest elevation 834.0m, max height 289.0m), flood discharge structures, and power generation system. The dam features a 13m-wide crown beam, 72m base width, and

arc-height ratio of 2.63. The underground powerhouses are symmetrically placed on both riverbanks, with a tailrace system of four tunnels per bank (two units per tunnel). Five diversion tunnels (left bank: 1–3; right bank: 4–5; total length 8,980 m) were constructed via cofferdams and tunnel diversion. These double-curved tunnels are spaced 60 m apart (75 m upstream on the right bank) and link downstream to tailrace tunnels 2–5. Table 1 details right bank tunnel specifications. Table 1 shows the basic specifications for the right bank tunnels.

Table 1

**Basic conditions of diversion tunnel on the right bank**

	Elevation (m)[In/Out]	Length (m)	Tailwater section(m)	Section (m)	Type
4#	585.00/574.00	1650.87	351.88	17.5×22.0	Round arch straight wall
5#	605.00/574.00	1945.63	439.66	17.5×22.0	

Using the WBS-RBS method, 18 risk factors were identified for the 5# diversion tunnel. Probability distributions were simulated using field data and validated via hypothesis testing. Fig. 9 shows resettlement issues (R16) fitting results, while Fig. 10 compares cumulative growth curves vs. log-normal distribution.

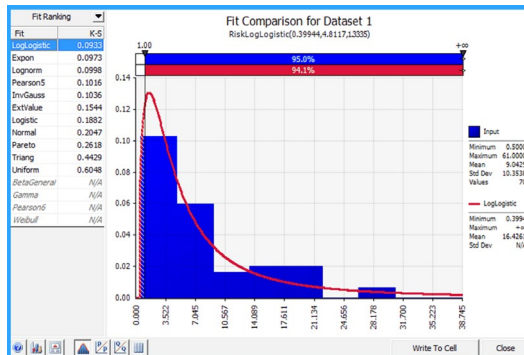


Fig. 9. Fitting results of R16

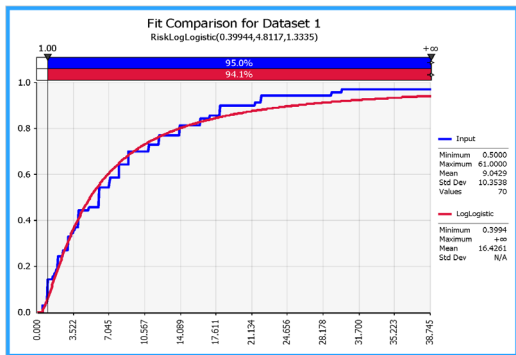


Fig. 10. Comparison of cumulative growth curve and log-normal distribution

Similarly, probability distributions of other risk factors were determined by fitting actual construction records and historical data. Research findings from literature were synthesized, with assumptions made for risk factors lacking empirical data. Table 2 summarizes the results.

Table 2

**Summary of risk factors obeying probability distribution type**

<b>Risk factors</b>	<b>Probability distribution types</b>
Physiological status (R1)	Binomial Distribution
Psychological state (R2)	Binomial Distribution
Construction skills (R3)	Log-normal Distribution
Faults in large-scale mechanical equipment (R4)	Bernoulli Distribution
Insufficient supply of blasting materials (R5)	Uniform Distribution
Equipment transportation, installation, disassembly and commissioning (R6)	Exponential Distribution
Dimension and quality issues of prefabricated materials (R7)	Log-normal Distribution
Blockage in anchor grouting pipelines (R8)	Poisson Distribution
Poor geological conditions (R9)	Triangular Distribution
Geological hazards (R10)	Gamma Distribution
Meteorology and hydrology (R11)	Pearson-III Distribution
Tunnel road blockage (R12)	Poisson Distribution
Interruption of wind, water and electricity for construction (R13)	Log-normal Distribution
Risk of elevated temperatures, dust, open flames and other hazards (R14)	Log-normal Distribution
Construction interference (R15)	Trapezoidal Distribution
Resettlement issues (R16)	Inverse Gaussian Distribution
Improper construction organization (R17)	Triangular Distribution
Design alteration (R18)	Uniform Distribution

**4.1. Homogeneous single-factor coupling**

Monte Carlo simulations analyzed construction timelines and active risk factors for the 5# diversion tunnel, determining extreme and mean values for individual risks. Results are shown in Fig. 11. Efficacy coefficients were calculated using Eq. (2), while homogeneous risk coupling strengths were computed via Eq. (1), ranked by intensity. Table 3 lists ranked results.

The analysis of homogeneous coupling strengths identifies critical risk pairings and provides actionable insights for management. For M<sub>1</sub>, the dominant coupling between R1 and R3 underscores how personnel well-being directly impacts operational proficiency. In the M<sub>2</sub> category, R4 drives the strongest couplings, highlighting the critical need for equipment reliability. Among E, R9, R10 and R12 are the most severe. Finally, M<sub>3</sub> risks show exceptionally strong coupling (R17-R18), indicating that organizational and design decisions are highly

interdependent. These findings allow managers to move beyond single-risk prevention to proactively mitigate high-risk combinations.

Table 3

Calculation table of homogeneous single-factor coupling strength

	Risk factor	Completion probability	Minimum (Day)	Maximum (Day)	Mean value (Day)	Efficiency coefficient-U	Coupling strength $qd_{ij}$
M <sub>1</sub>	R1	82.9%	781.13	788.13	785.00	0.4444	0.49772 (R1-R3) 0.49739 (R1-R2) 0.49035 (R2-R3)
	R2	89.5%	779.63	785.63	782.75	0.5454	
	R3	79%	780.74	791.26	784.25	0.3671	
M <sub>2</sub>	R4	73.5%	782.88	790.88	786.50	0.4650	0.4998 (R4-R8) 0.4997 (R4-R7) 0.39065 (R6-R7) 0.38219 (R4-R6)
	R5	85%	776.07	797.90	787.00	0.4991	
	R6	92.3%	776.00	811.96	779.27	0.1004	
	R7	94.6%	781.35	787.10	783.75	0.4340	
	R8	70.2%	781.25	789.63	784.75	0.4923	
E	R9	87.8%	781.02	787.61	784.25	0.4659	0.49989 (R9-R10) 0.49987 (R10-R12) 0.49962 (R12-R15) 0.49782 (R10-R14) 0.49646 (R12-R14) 0.49646 (R13-R16) 0.45934 (R11-R13) 0.37058 (R10-R11) 0.29079 (R13-R14) 0.27437 (R12-R13) 0.26910 (R10-R13) 0.23956 (R15-R16)
	R10	78.1%	781.63	789.25	785.25	0.4857	
	R11	88.2%	776.06	796.38	777.37	0.0955	
	R12	70.2%	779.38	787.00	783.00	0.4638	
	R13	93.5%	776.04	797.21	777.00	0.0414	
	R14	91.3%	780.84	785.99	783.02	0.4028	
	R15	79.3%	776.13	789.91	783.00	0.5011	
	R16	92.4%	776.06	815.96	778.16	0.0326	
M <sub>3</sub>	R17	82.9%	781.04	786.53	783.50	0.5056	0.49997 (R17-R18)
	R18	75.1%	776.50	792.52	784.44	0.4953	

#### 4.2 Heterogeneous multi-factor coupling

When factors from different subsystems act on the same process simultaneously, heterogeneous multi-factor coupling may occur. The Monte Carlo method simulates the overall construction duration of the #5 diversion tunnel under various risk coupling scenarios, with selected results shown in Fig. 12-Fig. 14.

The severity and uncertainty of schedule delays increase significantly as more risk categories are coupled. To quantify this effect, the coupling degree ( $T$  value) for each heterogeneous combination was calculated using the N-K model, with the results summarized in Table 4.

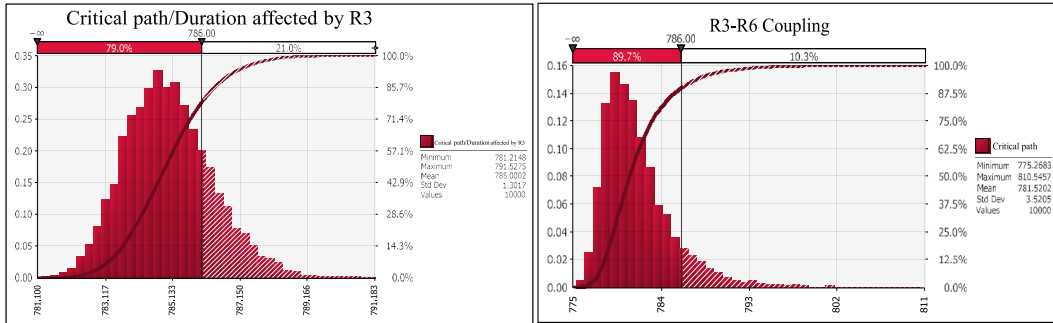


Fig. 11. Distribution and cumulative curve of the total construction period of critical path under the influence of R3

Fig. 12. Duration distribution of tunnel 5# under the R3-R6 coupling

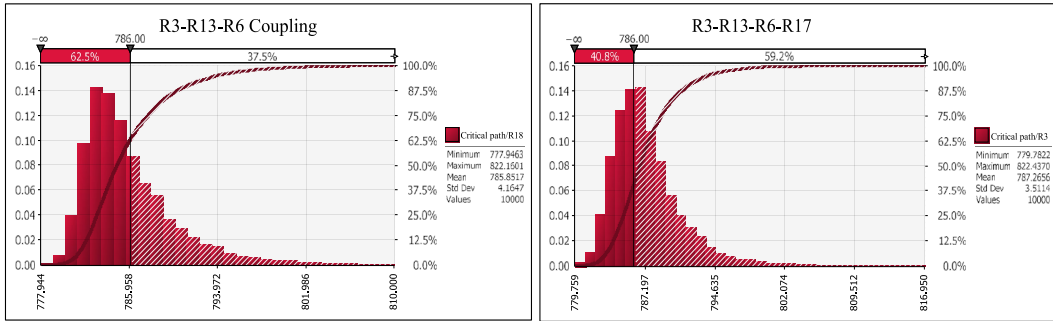


Fig. 13. Duration distribution of tunnel 5# under the R3-R13-R6 coupling

Fig. 14. Duration distribution of tunnel 5# under the R3-R13-R6-R17 coupling

Table 4

Table of  $T$  value

Coupling	$T$ value	Coupling	$T$ value	Coupling	$T$ value
$T_4(M_1-M_2-E-M_3)$	0.5250	$T_{33}(M_1-E-M_3)$	0.3119	$T_{21}(M_1-M_2)$	0.2567
$T_{32}(M_1-M_2-M_3)$	0.4066	$T_{23}(M_1-M_3)$	0.28683	$T_{24}(M_2-E)$	0.2499
$T_{34}(M_2-E-M_3)$	0.3487	$T_{26}(E-M_3)$	0.2763	$T_{22}(M_1-E)$	0.1078
$T_{31}(M_1-M_2-E)$	0.3415	$T_{25}(M_2-M_3)$	0.2589		

Schedule risk escalates with risk element quantity: 4-factor couplings > 3-factor > 2-factor, consistent with observed tunnel construction patterns.

For heterogeneous multi-factor coupling:  $M_1-M_2-M_3$  shows the highest risk. Subjective risks ( $M_1, M_3$ ) strongly couple with objective risks ( $M_2$ ) due to operational interdependencies. Environmental risks (E) demonstrate weaker coupling with subjective factors due to their independent occurrence. Specifically:  $M_1-M_3 > E-M_3 > M_2-M_3 > M_2-E > M_1-E$ . This highlights critical  $M_1-M_3$  linkages, where personnel errors ( $M_1$ ) can compound the effects of inadequate planning ( $M_3$ ).

## 5. Conclusions

This study developed an integrated schedule risk analysis model for diversion tunnels, combining WBS-RBS decomposition with SD. Key risk factors and their coupling mechanisms were quantified through three core findings:

(1) WBS-RBS identified 18 critical risks. SD causality diagrams revealed subjective risks (e.g., managerial decisions) and objective risks (e.g., environmental conditions) synergistically amplify delays through complex couplings.

(2) N-K models quantified homogeneous single-risk and heterogeneous multi-risk couplings. To address the challenge of obtaining historical data for N-K parameters, Monte Carlo simulations generated probability distributions for total construction duration and completion likelihood, enabling empirical determination of coupling parameters.

(3) Analysis of real-world project data demonstrated that increased risk types elevate coupling severity. Subjective risks (e.g.,  $M_1, M_3$ ) exhibited strong coupling with operational factors (e.g.,  $M_2$ ), leading to significant delays. While environmental risks showed weaker coupling with subjective factors, their standalone impact remained substantial, necessitating targeted mitigation.

The proposed model effectively identifies dominant risk factors and high-risk combinations, providing a structured framework for managers to optimize schedule control and enhance decision-making in diversion tunnel projects.

## Acknowledgments

This research was funded by National Natural Science Foundation of China (Grant No. 51879147, 52009069) and Open Fund of Hubei Key Laboratory of Construction and Management in Hydropower Engineering (Grant No. 2020KSD14, 2024KSD18).

## R E F E R E N C E S

- [1]. *A. Afshar, A. Barkhordary, A. Mariño*, Optimizing river diversion under hydraulic and hydrologic uncertainties, *Journal of Water Resources Planning and Management*, **vol. 120**, no. 1, 36-47, 1994.
- [2]. *M. Sari, AS. Selcuk, C. Karpuz, et al.*, Stochastic modeling of accident risks associated with an underground coal mine in Turkey, *Safety science*, **vol. 47**, no. 1, 78-87, 2009.
- [3]. *MM. Fouladgar, A. Yazdani-Chamzini, EK. Zavadskas*, Risk evaluation of tunneling projects, *Archives of civil and mechanical engineering*, **vol. 12**, no. 1, 1-12, 2012.
- [4]. *E. Eshtehardian, S. Khodaverdi*, A Multiply Connected Belief Network approach for schedule risk analysis of metropolitan construction projects, *Civil Engineering and Environmental Systems*, **vol. 33**, no. 3, 227-246, 2016.
- [5]. *D. Yi, EB. Lee, J. Ahn*, Onshore oil and gas design schedule management process through time-impact simulations analyses, *Sustainability*, **vol. 11**, no. 6, 1613, 2019.
- [6]. *A. Alitabar, R. Noorzad, A. Qolinia*, Evaluation of the instability risk of the dam slopes simulated with monte Carlo method (case study: Alborz Dam), *Geotechnical and Geological Engineering*, **vol. 39**, no. 6, 4237-4251, 2021.
- [7]. *N. Belu, DC. Anghel, N. Rachieru*, Failure Mode and Effects Analysis on control equipment using fuzzy theory, *Advanced Materials Research*, **vol. 837**, 16-21, 2014.

- [8]. *SH. Zyoud, D. Fuchs-Hanusch*, An integrated decision-making framework to appraise water losses in municipal water systems, *International Journal of Information Technology & Decision Making*, **vol. 19**, no. 05, 1293-1326, 2020.
- [9]. *F. Mohammadhasani, A. Pirouzmani*, Multi-state risk-based maintenance analysis of redundant safety systems using the Markov model and fault tree method, *Frontiers in Energy Research*, **vol. 9**, 685634, 2021.
- [10]. *V. Terzic, PK. Villanueva*, Method for probabilistic evaluation of post-earthquake functionality of building systems, *Engineering Structures*, **vol. 241**, 112370, 2021.
- [11]. *J. Zhang, J. Kang, L. Sun, et al.*, Risk assessment of floating offshore wind turbines based on fuzzy fault tree analysis, *Ocean Engineering*, **vol. 239**, 109859, 2021.
- [12]. *J. Yao, Y. Huang, K. Cheng*, Coupling effect of building design variables on building energy performance, *Case Studies in Thermal Engineering*, **vol. 27**, 101323, 2021.
- [13]. *T. Ji, JW. Liu, QF. Li*, Safety Risk Evaluation of Large and Complex Bridges during Construction Based on the Delphi-Improved FAHP-Factor Analysis Method, *Advances in Civil Engineering*, **vol. 2022**, no. 1, 5397032, 2022.
- [14]. *JN. Duressa, MS. Regasa*, Flood inundation mapping and risk analysis case of finchaa lake, *American Journal of Environmental Science and Engineering*, **vol. 5**, no. 3, 53-62, 2021.
- [15]. *Z. Xu, J. Yu, H. Li*, Analyzing Integrated Cost-Schedule Risk for Complex Product Systems R&D Projects, *Journal of Applied Mathematics*, **vol. 2014**, no. 1, 472640, 2014.
- [16]. *Y. Wu, LY. Zhao, YX. Jiang, et al.*, Research and application of intelligent monitoring system platform for safety risk and risk investigation in urban rail transit engineering construction, *Advances in Civil Engineering*, **vol. 2021**, no. 1, 9915745, 2021.
- [17]. *CZ. Li, J. Hong, F. Xue, et al.*, Schedule risks in prefabrication housing production in Hong Kong: A social network analysis, *Journal of cleaner production*, **vol. 134**, 482-494, 2016.
- [18]. *J. Birkmann*, Regulation and coupling of society and nature in the context of natural hazards, *Coping with global environmental change, disasters and security: Threats, challenges, vulnerabilities and risks*, Springer Berlin Heidelberg, **vol. 2011**, 1103-1127, 2011.
- [19]. *P. Brooker*, Air Traffic Management accident risk. Part 1: The limits of realistic modelling, *Safety science*, **vol. 44**, no. 5, 419-450, 2006.
- [20]. *S. Gomathi, Linda P E*. Interaction Coupling: A Modern Coupling Extractor, *Computational Intelligence, Cyber Security and Computational Models: Proceedings of ICC3*, **vol. 2013**, 237-244, 2013.
- [21]. *G. Xue, H. Wen*, Crash-Prone Section Identification for Mountainous Highways Considering Multi-Risk Factors Coupling Effect, *Journal of advanced transportation*, **vol. 2019**, no. 1, 9873832, 2019.
- [22]. *C. Jin, J. Liu, Z. Wang, et al.*, Early Cracking Risk Prediction Model of Concrete under the Action of Multifield Coupling, *Advances in Materials Science and Engineering*, **vol. 2021**, no. 1, 9920945, 2021.
- [23]. *F. Li, W. Wang, S. Dubljevic, et al.*, Analysis on accident-causing factors of urban buried gas pipeline network by combining DEMATEL, ISM and BN methods, *Journal of Loss Prevention in the Process Industries*, **vol. 61**, 49-57, 2019.
- [24]. *Z. Liu, X. Meng, Z. Xing, et al.*, Digital twin-based safety risk coupling of prefabricated building hoisting, *Sensors*, **vol. 21**, no. 11, 3583, 2021.
- [25]. *Y. Wang, L. Hou, M. Li, et al.*, A novel fire risk assessment approach for large-scale commercial and high-rise buildings based on fuzzy analytic hierarchy process (Fahp) and coupling revision, *International journal of environmental research and public health*, **vol. 18**, no. 13, 7187, 2021.